

A state change in the low-mass X-ray binary XSS J12270–4859

C. G. Bassa^{1*}, A. Patruno^{2,1}, J. W. T. Hessels^{1,3}, E. F. Keane^{4,5}, B. Monard⁶,
E. K. Mahony¹, S. Bogdanov⁷, S. Corbel⁸, P. G. Edwards⁹, A. M. Archibald¹,
G. H. Janssen¹, B. W. Stappers¹⁰, S. Tendulkar¹¹

¹*ASTRON, the Netherlands Institute for Radio Astronomy, Postbus 2, 7990 AA, Dwingeloo, the Netherlands*

²*Leiden Observatory, Leiden University, Postbus 9513, 2300 RA, Leiden, the Netherlands*

³*Astronomical Institute ‘Anton Pannekoek’, University of Amsterdam, Postbus 94249, 1090 GE, Amsterdam, the Netherlands*

⁴*Centre for Astrophysics and Supercomputing, Swinburne University of Technology, Mail H30, PO Box 218, VIC 3122, Australia*

⁵*ARC Centre of Excellence for All-Sky Astrophysics (CAASTRO)*

⁶*Kleinkaroo Observatory, Center for Backyard Astrophysics Kleinkaroo, Sint Helena 1B, PO Box 281, Calitzdorp 6660, South Africa*

⁷*Columbia Astrophysics Laboratory, Columbia University, 550 West 120th Street, New York, NY 10027, USA*

⁸*CEA, CNRS, Université Paris Diderot, Sorbonne Paris Cité, AIM, UMR 7158, DSM, IRFU, SAp, F-91191 Gif sur Yvette, France*

⁹*CSIRO Astronomy and Space Science, Australia Telescope National Facility, P.O. Box 76, Epping, NSW 1710, Australia*

¹⁰*Jodrell Bank Centre for Astrophysics, School of Physics and Astronomy, The University of Manchester, Manchester M13 9PL, UK*

¹¹*Space Radiation Laboratory, California Institute of Technology, 1200 E California Blvd, MC 249-17, Pasadena, CA 91125, USA*

Accepted 5 February 2014. Received 5 February 2014; in original form 5 February 2014

ABSTRACT

Millisecond radio pulsars acquire their rapid rotation rates through mass and angular momentum transfer in a low-mass X-ray binary system. Recent studies of PSR J1824–2452I and PSR J1023+0038 have observationally demonstrated this link, and they have also shown that such systems can repeatedly transition back-and-forth between the radio millisecond pulsar and low-mass X-ray binary states. This also suggests that a fraction of such systems are not newly born radio millisecond pulsars but are rather suspended in a back-and-forth state switching phase, perhaps for giga-years. XSS J12270–4859 has been previously suggested to be a low-mass X-ray binary, and until recently the only such system to be seen at MeV–GeV energies. We present radio, optical and X-ray observations that offer compelling evidence that XSS J12270–4859 is a low-mass X-ray binary which transitioned to a radio millisecond pulsar state between 2012 November 14 and 2012 December 21. Though radio pulsations remain to be detected, we use optical and X-ray photometry/spectroscopy to show that the system has undergone a sudden dimming and no longer shows evidence for an accretion disk. The optical observations constrain the orbital period to 6.913 ± 0.002 hr.

Key words: stars: individual: XSS J12270–4859 – stars: neutron – X-rays: binaries – binaries: general

1 INTRODUCTION

Low-mass X-ray binaries (LMXBs) are systems in which a neutron star or black hole is orbited by a Roche-lobe-filling, main-sequence companion with a mass $\lesssim 1 M_{\odot}$. In systems with neutron star primaries the accretion disk can transfer both matter and angular momentum to the neutron star, thereby spinning it up and eventually producing a “recycled” millisecond radio pulsar (MSP; Alpar et al. 1982; Radhakrishnan & Srinivasan 1982). The LMXB-MSP evolu-

tionary link has been demonstrated by, e.g., (i) the observation of accretion-powered pulsations in SAX J1808.4–3658 (Wijnands & van der Klis 1998); (ii) the discovery of the MSP PSR J1023+0038, a system in which an accretion disk was previously observed (Archibald et al. 2009); and (iii) the transition of PSR J1824–2452I/IGR J18245–245 from an MSP to an accreting X-ray millisecond pulsar (AMXP) and back (Papitto et al. 2013a). More recently, PSR J1023+0038 has re-entered a radio-quiet, accretion-disk state which shows much of the same X-ray and optical phenomenology observed in PSR J1824–2452I (Stappers et al. 2013; Takata et al. 2013; Patruno et al. 2014) — though the

* email: bassa@astron.nl

system has not yet entered a state of full accretion onto the neutron star surface. As such, we have witnessed a growing number of systems that straddle the classical definitions of LMXB and MSP, and which are helping us map this interesting evolutionary phase.

In addition to the aforementioned systems, recent radio pulsar searches have identified dozens of new “black widow” and “redback” systems (Roberts 2013). These are compact radio pulsar binary systems in which eclipsing of the pulsed signal is normally observed around superior conjunction of the neutron star, indicating that material is actively being ablated from the companion by the pulsar wind. The black widow systems are those in which the companion is very low mass ($\sim 0.01 M_{\odot}$) and, likely degenerate. The redbacks have likely non-degenerate companions that are significantly more massive (about 0.1 to $0.7 M_{\odot}$). The rapid growth in the known population of such sources has come from deep, targeted radio pulsation searches towards Galactic globular clusters (e.g. Ransom et al. 2005; Hessels et al. 2007) as well as towards unidentified γ -ray sources found with the *Fermi Gamma-ray Space Telescope* (Ray et al. 2012). Since SAX J1808.4–3658, PSR J1023+0038 and PSR J1824–2452I can all be classified as belonging to the black widow or redback families (though SAX J1808.4–3658 has never been seen to pulse in radio it has shown evidence that a radio pulsar is active during the X-ray quiescent phase, see Burderi et al. 2003 and Campana et al. 2004), it seems likely that in the coming decade some of these other, newly found MSPs will also be seen to transition to an X-ray active phase and back. In fact, one may ponder whether these systems are gradually making a definitive transition from LMXB to MSP, or whether they are stuck transitioning back and forth for many giga-years (see Chen et al. 2013 for evolutionary modeling of such systems).

PSR J1023+0038’s recent transition back to an LMXB-like state — in which an accretion disk has returned (Patruno et al. 2014) — has been accompanied by an additional observational surprise: namely that the MeV-GeV brightness of the system has quintupled in concert with the disappearance of the radio pulsar (Stappers et al. 2013). The emission of γ -rays is somewhat unexpected in LMXBs, and is more commonly seen in X-ray binaries with O or B-type companions in much wider orbits (Dubus 2013). This is the first time that γ -ray variability has been observed in an LMXB/MSP system, and it provides a new diagnostic tool while also raising new questions about the origin of this high-energy emission.

Prior to the increase of the PSR J1023+0038 system’s γ -ray flux, the only LMXB thought to emit γ -rays was XSS J12270–4859. Discovered in the RXTE slew survey (Sazonov & Revnivtsev 2004), this system was initially classified as an $R = 15.7$ cataclysmic variable by Masetti et al. (2006), based on the presence of optical emission lines. Follow-up optical and X-ray observations cast doubt on this classification, suggesting instead that it is an LMXB (Pretorius 2009; Saitou et al. 2009; de Martino et al. 2010). Subsequently, de Martino et al. (2010) and Hill et al. (2011) noted the positional coincidence of XSS J12270–4859 with the *Fermi* γ -ray source 1FGL J1227.9–4852 (2FGL J1227.7–4853). Based on that coincidence and similarities with PSR J1023+0038, Hill et al. (2011), de Martino et al. (2013a) and Papitto et al.

(2013b) suggested that also XSS J12270–4859 could harbour an active radio MSP.

Here we present radio, optical and X-ray observations to expand on our earlier report (Bassa et al. 2013) where we suggested that XSS J12270–4859 has recently undergone a state transition similar to that observed in PSR J1023+0038. In the case of XSS J12270–4859, however, it appears that the system has transitioned from an LMXB-like state to a radio MSP-like state, i.e. the opposite switch that PSR J1023+0038 has recently made (Stappers et al. 2013). In §2 we present our observations and analysis, in §3 our results, and end with a discussion in §4.

2 OBSERVATIONS AND ANALYSIS

2.1 Optical

XSS J12270–4859 has been monitored at optical wavelengths with a roughly monthly cadence or better since 2007. Observations were carried out at the Bronberg (2007-2010) and Kleinkaroo Observatories (2011-2013) in South Africa. Unfiltered magnitudes were obtained with Meade RCX 400 telescopes, having apertures of 30 and 35 cm and working at F/8, and an SBIG ST8-XME CCD camera, using 2×2 spatial binning and averages of 3 to 5 exposures of 13 s each. The CCD camera has a quantum efficiency of 50% to 90% over the 4500 to 8000 Å wavelength range, roughly covering the Johnson *V* and *R*-band filters. The light-curve is shown in Fig. 1.

We obtained optical spectroscopy of XSS J12270–4859 with EFOSC2, the ESO Faint Object Spectrograph and Camera, at the NTT on La Silla in Chile on 2013 November 8. The sky was clear with $1''$ seeing. Two 900-s exposures were obtained with a $1''$ slit in combination with grism #18, giving a wavelength coverage of 4720 to 6730 Å. With 2×2 binning, this is sampled at 2.0 \AA pix^{-1} and provides a resolution of 8.4 Å. The observations were corrected for bias offsets and the sky background was subtracted using clean regions offset from the spectral trace. The spectra were extracted using the optimal extraction method of Horne (1986) and wavelength calibrated using arc lamp exposures. Flux calibration was performed against the Feige 110 spectrophotometric flux standards. The calibration is approximate as no attempt was made to correct for slit losses. Figure 2 shows the average of the two 900 s spectra.

These ground-based optical data were complemented by eleven pointed observations made with the *Swift*/Ultra-Violet and Optical Telescope (UVOT; Roming et al. 2005). The first observation was taken on 2013 January 26, whereas the next ten were collected between 2013 December 10 and 2014 January 8. Each of the latter ten observations consists of one to three exposures, all taken with the *U*-band filter (central wavelength of 3465 Å). The 2013 January observation instead comprises six short snapshots recorded with each of the six optical and UV filters. A visual inspection of the images reveals a dim counterpart in all the *U*-band filter observations and a lack of counterpart in five of the six short snapshots of January 26 (only the *B*-band filter counterpart is clearly seen).

We extracted the source magnitude using the standard UVOT pipeline and selected the photons coming from a region of $3 - 4''$ centered on the pixel with the highest count

rate (and compatible, within uncertainties, with the known source position of Masetti et al. 2006). The background is extracted from a circular region with radius of $20''$, positioned in a location free from bright sources. We extracted the magnitudes with two methods: in the first method, we summed all the single exposures comprised in each observation with the `uvotimsum` tool to obtain the highest possible signal-to-noise ratio and extracted the magnitudes with the `uvotsource` tool (distributed with the `heasoft` v.6.14). The second method uses the tool `uvotmagnhist` to extract the magnitudes from each single exposure and follow the source brightness variations on a timescale of hours.

We also make use of recently acquired data using the *XMM-Newton* Optical Monitor (OM) data; the corresponding EPIC X-ray data set will be presented elsewhere. *XMM-Newton* observed XSS J12270–4859 as a target of opportunity starting on 2013 December 29 for a total duration of 38 ks. The OM was configured in fast mode to permit rapid photometry using the *U*-band filter. Ten exposures of 3 ks were acquired. The data were processed using the `omfchain` pipeline in SAS¹ version `xmmsas_20130501_1901-13.0.0` using the default parameters.

2.2 X-ray

The same eleven *Swift* observations, plus five additional ones, were used to extract the X-ray data recorded with the X-Ray Telescope (XRT). The additional observations refer to the period from 2012 August to September. Each of the 17 observations lasted for 0.5–2.5 ks and the XRT operated exclusively in PC mode with a time resolution of approximately 2.5 s. A number of additional *Swift*/XRT observations were collected between 2005 and 2011; their analysis was previously reported in de Martino et al. (2013a) and Tam et al. (2013).

The data were analyzed using the XRT pipeline and by applying standard screening criteria. We extracted all photons with an energy between 0.3–10 keV that fall within an extraction region of $15-40''$. The center of the extraction region is centered on the pixel with the highest count rate and is compatible with the best astrometric position available (Masetti et al. 2006). We then extracted the background by selecting a region with a radius two times the source extraction region size, randomly placed but in locations far from known X-ray sources. The count rate was corrected for the presence of bad pixels, vignetting and dead columns, and normalized to match the source region area. We then repeated the entire procedure by using the `detect` and `sosta` FTOOLS² under the `ximage` package (v.4.5.1) and obtained consistent results. For the non-detections, 95% upper limits are given, calculated according to the prescription given in Gehrels (1986). The small number of photons prevented the fit of the X-ray spectrum but the count-rate is consistently below, at least by an order-of-magnitude, that reported in

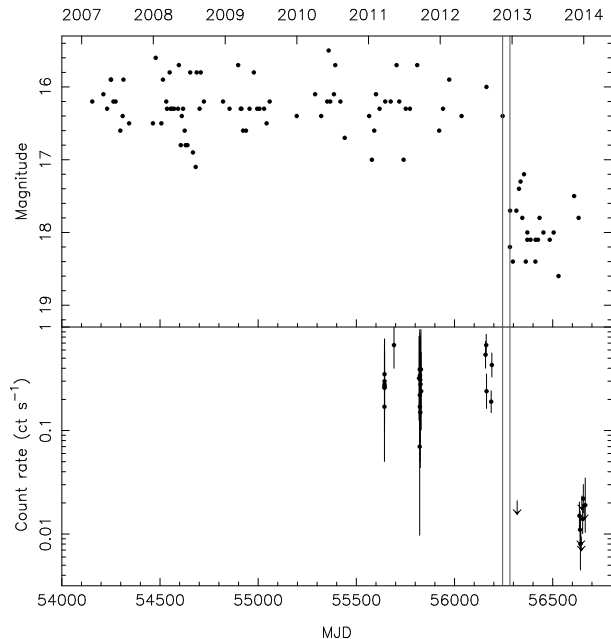


Figure 1. *Top panel:* The long-term optical light-curve of XSS J12270–4859 obtained from the Bronberg and Kleinkaroo Observatories. Unfiltered magnitudes were determined from images obtained with the same telescope and CCD camera combination over the 6-year period. Typical magnitude uncertainties range from 0.02 mag at 16th magnitude to 0.25 mag at 19th magnitude. A 1.5 to 2 mag decrease in brightness occurred between 2012 November 14 and 2012 December 21. That time period is indicated with the vertical lines. *Bottom panel:* *Swift*/XRT long-term light-curve of XSS J12270–4859 in the 0.3–10 keV energy band. The plot shows an order-of-magnitude decrease in the X-ray count rate that is qualitatively consistent with the decrease in optical brightness. The data prior to 2012 are taken from de Martino et al. (2013a).

de Martino et al. (2010, 2013a) in all eleven observations recorded after 2012 December.

2.3 Radio

A faint, continuum radio source has previously been associated with XSS J12270–4859 (Hill et al. 2011). In order to probe its variability, we conducted a new radio observation with the Australia Compact Array Telescope (ATCA) located near Narrabri (Australia), on 2013, December 17. The observations were conducted at 5.5 and 9 GHz in the 750B array configuration with the upgraded and sensitive CABB back-end (Wilson et al. 2011) for a total time on source of 5.48 hours. The amplitude and band-pass calibrator was PKS 1934–638, and the antennas’ gain and phase calibration, as well as the polarization leakage, were derived from regular observations of the nearby calibrator PMN J1326–5256. The editing, calibration, Fourier transformation with multifrequency algorithms, deconvolution, and image analysis were performed using the MIRIAD software package (Sault & Killeen 1998).

Furthermore, we searched for radio pulsations using the 64-m Parkes radio telescope. Observations were acquired at 1.4 GHz using the central beam of the multi-beam receiver (pointing position: $\alpha_{J2000} = 12^{\text{h}}27^{\text{m}}58^{\text{s}}.68$, $\delta_{J2000} =$

¹ The *XMM-Newton* SAS is developed and maintained by the Science Operations Centre at the European Space Astronomy Centre and the Survey Science Centre at the University of Leicester.

² <http://heasarc.gsfc.nasa.gov/ftools/>

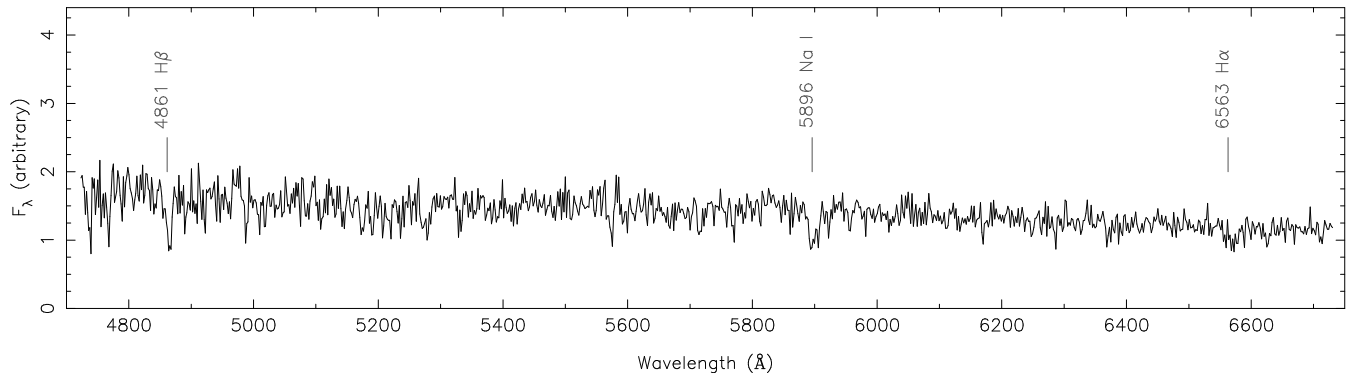


Figure 2. The average optical spectrum of XSS J12270–4859 obtained with EFOSC2 at the NTT on 2013 November 8 (orbital phase of $\phi = 0.66$). Obvious spectral lines are indicated. The spectral type is consistent with late-G/early-K.

–48°53′42″.0). Summed polarization, filterbank data were recorded as 2-bit samples over a 400-MHz bandwidth, of which 340 MHz is usable, using the BPSR backend (Keith et al. 2010), which provided 0.39-MHz channels and 64- μ s time resolution. XSS J12270–4859 was observed for 5 hrs on 2013 November 13 and for 1 hr on 2013 November 17.

Using the PRESTO³ pulsar search suite, we excised radio frequency interference (RFI) and performed an acceleration search (Ransom et al. 2002) for spectral drifts between $-500 < z < 500$ bins, as well as trial dispersion measures (DMs) between $0 - 300 \text{ pc cm}^{-3}$ (in steps of 0.1 pc cm^{-3}). The highest trial DM was chosen to be $2\times$ larger than the maximum expected DM along this line-of-sight, according to the NE2001 model of the Galactic free electron density (Cordes & Lazio 2002). If XSS J12270–4859 is at 1.4–3.6 kpc, as estimated by de Martino et al. (2013a), then the model predicts a DM in the range of 30 to 100 pc cm^{-3} . For $\text{DM} = 100 \text{ pc cm}^{-3}$, the intra-channel dispersion smearing at the lowest observed frequency is 200 μ s. Acceleration search processing gives improved sensitivity to periodic signals that are Doppler shifted by orbital motion, but it assumes a linear drift of the signal in the power spectrum and thus is only valid when the observation time, T_{obs} , is $\lesssim 0.1P_{\text{orb}}$, the orbital period (Ransom et al. 2002). Given the proposed 6.913-hr orbital period (see §3), we searched the data in 10 and 32-minute chunks, in order to remain in the constant acceleration regime. The resulting candidates were sifted to look for signals that showed a peak in signal-to-noise ratio with DM. Promising candidates were folded at the candidate rotational period and DM, in order to create a full diagnostic plot. The likelihood that the resulting signals were astrophysical in origin was then judged based on a range of standard criteria (Hessels et al. 2007).

3 RESULTS

The optical and X-ray observations presented here allow us to study the behaviour of XSS J12270–4859 on long as well as short time scales. Figure 1 shows the long-term optical and X-ray light-curves of XSS J12270–4859. Both light-curves show a sudden decrease in brightness, where the de-

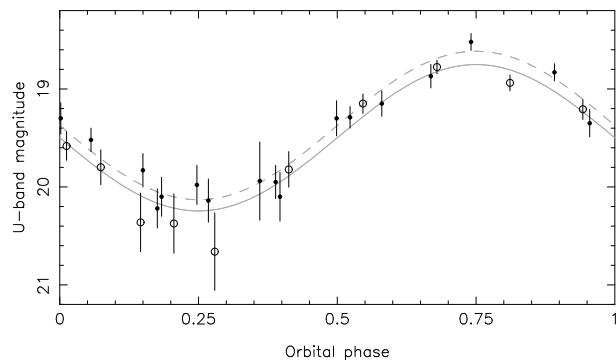


Figure 3. The *U*-band magnitudes observed by *Swift*/UVOT from 2013 December 10 to 2014 January 8 (solid points) and by *XMM-Newton*/OM on 2013 December 29/30 (open points). The data are folded at the best fit orbital period, and the dashed and solid lines show the best fit amplitude and mean for *Swift*/UVOT and *XMM-Newton*/OM, respectively. The curves are offset since the data of each instrument was allowed to have a different mean and amplitude while fitting for the same orbital period and phase.

crease appears to have occurred between 2012 November 14 and 2012 December 21. A decrease of 1.5 to 2 mag is seen in the optical, while the X-ray light-curve shows that the *Swift*/XRT count rate decreased by at least a factor of 10 over that same time period.

On shorter time scales, the 10-hr *U*-band light-curve obtained by *XMM-Newton*/OM shows sinusoidal variations at the 6.91-hr orbital period reported by de Martino et al. (2013b). The variability is also present in the *U*-band observations obtained with *Swift*/UVOT over the 29-day interval. By approximating the light-curves of both instruments with a sine and fitting for six parameters: period, phase, and, to allow for differences between the *U*-band filters, mean *U*-band magnitude and variability amplitude separately for each instrument, we obtain an orbital period of 6.913 ± 0.002 hr, with zero phase occurring at HJD 2456651.026 ± 0.002 . The χ^2 of the fit is 19.2 for 21 degrees of freedom. Figure 3 shows the *U*-band observations folded on this ephemeris. This orbital period is consistent, though an order-of-magnitude more accurate, with that reported by de Martino et al. (2013b).

The optical spectrum of XSS J12270–4859 obtained in 2013 November is shown in Fig. 2 and shows weak absorption

³ <http://www.cv.nrao.edu/~sransom/presto/>

lines of Hydrogen, as well as the sodium doublet. The spectrum does not have the signal-to-noise, nor covers a large enough spectral range, to determine accurate spectral parameters, but a comparison with template spectra from the library of Le Borgne et al. (2003) constrains the spectral type to late-G/early-K.

To estimate the X-ray luminosity we assume an absorbed power-law with a very low absorption column ($N_H \sim 10^{21} \text{ cm}^{-2}$), compatible with that estimated by de Martino et al. (2010), and spectral index $\Gamma = 1 - 2$. Given the source distance (1.4–3.6 kpc; de Martino et al. 2013a), this corresponds to an unabsorbed luminosity between $7 \times 10^{31} \text{ erg s}^{-1}$ and $4 \times 10^{32} \text{ erg s}^{-1}$. With the correspondingly low count rates, we cannot explore timescales shorter than the length of each observation ($\sim 1 \text{ ks}$). Furthermore, the small number of detections and low count rate are insufficient to study X-ray orbital modulation.

The 2013 December ATCA observations lead to no detection of the radio source that was previously found (Hill et al. 2011) at the location of XSS J12270–4859 with 3σ upper limits of $30 \mu\text{Jy}$ at 5.5 GHz and $33 \mu\text{Jy}$ at 9 GHz. A reanalysis of the 2010 radio flux densities presented in Hill et al. (2011), taking into account the primary beam correction, yields detections of $190 \pm 30 \mu\text{Jy}$ at 5.5 GHz and $180 \pm 40 \mu\text{Jy}$ at 9 GHz. This clearly indicates a significant reduction (by at least a factor of 6) of radio emission from XSS J12270–4859 in association with its recent state change.

The Parkes searches have thus far failed to identify a radio pulsar signal. In our 32-minute searches, we can infer a flux density upper limit of 0.2 mJy at 1.4 GHz, assuming a minimum detectable signal-to-noise $S/N_{\text{min}} = 10$ and a 20% duty cycle. This is comparable to the flux density limit reported during XSS J12270–4859’s previous state (Hill et al. 2011). The radio non-detection is discussed in more detail in §4.

4 DISCUSSION AND CONCLUSIONS

Our radio, optical, and X-ray observations show that, sometime between 2012 November 14 and 2012 December 21, XSS J12270–4859 transitioned to a new state where it is consistently and considerably fainter in these bands, and where the previous signs of an accretion disk (i.e. double-peaked optical emission lines) have disappeared. Subsequent to our report of this transition in Bassa et al. (2013), Tam et al. (2013) reported a similar decrease in brightness of XSS J12270–4859 in γ -rays, while Casares Velazquez et al. (2014) confirm the absence of emission lines at all orbital phases.

This phenomenology shows many parallels with PSR J1023+0038, which has recently transitioned from being a radio millisecond pulsar to a state where it resembles a quiescent LMXB (Archibald et al. 2009; Wang et al. 2009; Stappers et al. 2013; Takata et al. 2013; Patruno et al. 2014). Compared with PSR J1023+0038’s recent behaviour, however, the XSS J12270–4859 observations presented here strongly suggest the reverse transition, i.e. from an LMXB-like state in 2012 to one where the accretion disk is absent in 2013. Besides the presence of an accretion disk during the LMXB state, the XSS J12270–4859 X-ray light-curve

presented by de Martino et al. (2013a) displays frequent low flux states in brightness, similar to what is seen in the recent LMXB state of PSR J1023+0038 (Patruno et al. 2014) as well as during PSR J1824–2452I’s X-ray active phase (Papitto et al. 2013a). The cause of the low X-ray flux states in both systems is presently unknown. The sinusoidal U -band light-curve that is seen in the present state of XSS J12270–4859 is comparable to the light-curves presented in Woudt et al. (2004) and Thorstensen & Armstrong (2005) and can be understood as irradiation of the companion by the neutron star.

A radio source coincident with XSS J12270–4859 was detected by Hill et al. (2011) in ATCA observations obtained in 2009 when the source was in the LMXB state. Our follow-up ATCA observations obtained after the transition show it has decreased in brightness by at least a factor of 6. Recent Very Large Array observations of PSR J1023+0038 after it returned to the LMXB state show a flat spectrum radio source (Deller et al. in prep.). All these parallels between XSS J12270–4859 and PSR J1023+0038 lead us to conclude that XSS J12270–4859 harbours an active rotation-powered millisecond pulsar (see also Papitto et al. 2013b) and, based on the present information, one could classify XSS J12270–4859 as a “redback” system in its current state.

Thus far, however, we have failed to detect radio pulsations from XSS J12270–4859. Though such a detection would show without a doubt that the system has transitioned from an LMXB state to an MSP state, the lack of radio detection in no way rules out such a state transition. Given the high inferred mass ratio, $q = 0.53$ (de Martino et al. 2013b), it appears that XSS J12270–4859 would be observed as a redback in its present state. In analogy with other redback systems, we expect the pulsar to be eclipsed for $\sim 50\%$ of the time at $\sim 1.4 \text{ GHz}$, and it is possible that the system is enshrouded a much larger fraction of the time. Indeed, the recent examples of PSR J2339–0533 (Romani & Shaw 2011) and PSR J1311–3430 (Ray et al. 2013) show that the radio detectability of such pulsars may be exceedingly poor, even though the radio pulsar mechanism is clearly active. For this reason, continued radio pulsar searches may eventually be successful in detecting the source. It is also simply possible that the radio pulsar is too weak to detect with the current Parkes data, too highly accelerated without using a far more complex acceleration search, or not beamed towards the Earth.

PSR J1023+0038’s transition from MSP to LMXB was accompanied by a 5-fold increase in γ -ray flux (Stappers et al. 2013). Assuming that XSS J12270–4859 is mirroring such a transition, we would thus expect a marked decrease in γ -ray brightness. Using the optically and X-ray-derived epoch of the state change, Tam et al. (2013) report that the γ -ray brightness has indeed decreased by a factor of 1.5 to 2, but note that the decrease appears more gradual than what was seen in PSR J1023+0038. Indeed, the γ -ray light-curve of XSS J12270–4859 appears more complicated than that of PSR J1023+0038 and we are investigating whether there is contamination from another source.

PSR J1023+0038’s transition from radio MSP to LMXB is constrained to have happened within a 2-week window (Stappers et al. 2013), and may well have happened even more abruptly. XSS J12270–4859’s mirror transition from

LMXB to an MSP-like state is constrained to a 5-week period, and is thus also quite rapid. An additional comparison is provided by PSR J1824–2452I’s 2013 transition from accreting X-ray MSP to an observable radio MSP, within a period of less than 3 weeks. It thus appears that the back-and-forth transitioning of such systems between MSP and LMXB is a rapid process which high-cadence radio and X-ray monitoring can constrain further. In particular, though practically difficult to achieve, near-daily, joint radio and X-ray monitoring would either detect or strongly constrain whether there is a lag between the X-ray brightening and disappearance of the radio MSP.

Besides the similarities with PSR J1023+0038, there are also differences. XSS J12270–4859’s high reported mass ratio $q = 0.53$ (de Martino et al. 2013b) suggests a significantly more massive companion compared with PSR J1023+0038 ($M_c = 0.2 M_\odot$) and the majority of the other observed redbacks (see Roberts 2013 for a review). Such a high companion mass is not unprecedented, however; PSR J1723–2837 (Crawford et al. 2013) has an inferred $M_{c,\min} = 0.7 M_\odot$ companion and PSR J2129–0428 (Hessels et al., in prep.) has a $M_{c,\min} = 0.5 M_\odot$ companion. A much larger number of LMXB/MSP transition systems will have to be characterized before it is possible to determine the role that companion mass has on the frequency of state switches.

Thus far we have observed similar back-and-forth transitioning from three redbacks; PSR J1023+0038, PSR J1824–2452I, and now also in XSS J12270–4859. Should we expect the same from the black widows? For the accreting X-ray millisecond pulsars, roughly half have black-widow-like companions and half have redback-like companions (Patruno & Watts 2012). There is no obvious correlation between the recurrence timescales in such system and the companion mass. Why have such systems not been observed as radio pulsars? Possibly simply because they are mostly very distant, which is problematic both because radio MSPs are intrinsically quite faint and because distant sources at low Galactic latitudes will be scattered.

The observations and analysis presented in this paper show that XSS J12270–4859 has undergone a state transition similar to those observed in PSR J1023+0038 and PSR J1824–2452I. The analysis of recently obtained *XMM/Newton* and *Chandra* X-ray observations of XSS J12270–4859 may shed further light on the presence of an active radio MSP, though multiwavelength observations are certainly warranted. For example, the present absence of the accretion disk allows for optical spectroscopy of the main sequence companion. This will provide constraints on the masses of the companion and the neutron star. Finally, regular optical and X-ray will help identify future transitions, constraining the timescales involved in the transitions and possibly trigger detailed investigations during the transitions.

ACKNOWLEDGMENTS

C.G.B. acknowledges support from ERC Advanced Grant “LEAP” (227947, PI: Michael Kramer). A.M.A. and J.W.T.H. acknowledge support from a Vrije Competitie grant from NWO. J.W.T.H. and A.P. acknowledge support from NWO Vidi grants. J.W.T.H. also acknowledges fund-

ing from an ERC Starting Grant “DRAGNET” (337062). E.F.K. acknowledges the support of the Australian Research Council Centre of Excellence for All-sky Astrophysics (CAASTRO), through project number CE110001020. S.C. acknowledges the financial support from the UnivEarthS Labex program of Sorbonne Paris Cité (ANR-10-LABX-0023 and ANR-11-IDEX-0005-02). The Australia Telescope Compact Array and Parkes radio telescope are part of the Australia Telescope National Facility which is funded by the Commonwealth of Australia for operation as a National Facility managed by CSIRO. The work presented was based in part on observations obtained with *XMM-Newton*, an ESA science mission with instruments and contributions directly funded by ESA Member States and NASA.

REFERENCES

- Alpar M. A., Cheng A. F., Ruderman M. A., Shaham J., 1982, *Nat*, 300, 728
- Archibald A. M., Stairs I. H., Ransom S. M., Kaspi V. M., Kondratiev V. I., Lorimer D. R., McLaughlin M. A., Boyles J., Hessels J. W. T., Lynch R., van Leeuwen J., Roberts M. S. E., Jenet F., Champion D. J., Rosen R., Barlow B. N., Dunlap B. H., Remillard R. A., 2009, *Science*, 324, 1411
- Bassa C. G., Patruno A., Hessels J. W. T., Archibald A. M., Mahony E. K., Monard B., Keane E. F., Bogdanov S., Stappers B. W., Janssen G. H., Tendulkar S., 2013, *The Astronomer’s Telegram*, 5647, 1
- Burderi L., Di Salvo T., D’Antona F., Robba N. R., Testa V., 2003, *A&A*, 404, L43
- Campana S., D’Avanzo P., Casares J., Covino S., Israel G., Marconi G., Hynes R., Charles P., Stella L., 2004, *ApJ*, 614, L49
- Casares Velazquez J., de Martino D., Mason E., D’Avanzo P., Campana S., Fugazza S., Covino S., Belloni T., Munoz-Darias T., Cornelisse R., Nicastro L., 2014, *The Astronomer’s Telegram*, 5747, 1
- Chen H.-L., Chen X., Tauris T. M., Han Z., 2013, *ApJ*, 775, 27
- Cordes J. M., Lazio T. J. W., 2002, [astro-ph/0207156](#)
- Crawford F., Lyne A. G., Stairs I. H., Kaplan D. L., McLaughlin M. A., Freire P. C. C., Burgay M., Camilo F., D’Amico N., Faulkner A., Kramer M., Lorimer D. R., Manchester R. N., Possenti A., Steeghs D., 2013, *ApJ*, 776, 20
- de Martino D., Belloni T., Falanga M., Papitto A., Motta S., Pellizzoni A., Evangelista Y., Piano G., Masetti N., Bonnet-Bidaud J.-M., Mouchet M., Mukai K., Possenti A., 2013a, *A&A*, 550, A89
- de Martino D., Casares Velazquez J., Mason E., Kotze M., Buckley D. A. H., 2013b, *The Astronomer’s Telegram*, 5651, 1
- de Martino D., Falanga M., Bonnet-Bidaud J.-M., Belloni T., Mouchet M., Masetti N., Andruchow I., Cellone S. A., Mukai K., Matt G., 2010, *A&A*, 515, A25
- Dubus G., 2013, *A&AR*, 21, 64
- Gehrels N., 1986, *ApJ*, 303, 336
- Hessels J. W. T., Ransom S. M., Stairs I. H., Kaspi V. M., Freire P. C. C., 2007, *ApJ*, 670, 363

- Hill A. B., Szostek A., Corbel S., Camilo F., Corbet R. H. D., Dubois R., Dubus G., Edwards P. G., Ferrara E. C., Kerr M., Koerding E., Koziel D., Stawarz L., 2011, *MNRAS*, 415, 235
- Horne K., 1986, *PASP*, 98, 609
- Keith M. J., Jameson A., van Straten W., Bailes M., Johnston S., Kramer M., Possenti A., Bates S. D., Bhat N. D. R., Burgay M., Burke-Spolaor S., D’Amico N., Levin L., McMahan P. L., Milia S., Stappers B. W., 2010, *MNRAS*, 409, 619
- Le Borgne J.-F., Bruzual G., Pelló R., Lançon A., Rocca-Volmerange B., Sanahuja B., Schaerer D., Soubiran C., Vilchez-Gómez R., 2003, *A&A*, 402, 433
- Masetti N., Morelli L., Palazzi E., Galaz G., Bassani L., Bazzano A., Bird A. J., Dean A. J., Israel G. L., Landi R., Malizia A., Minniti D., Schiavone F., Stephen J. B., Ubertini P., Walter R., 2006, *A&A*, 459, 21
- Papitto A., Ferrigno C., Bozzo E., Rea N., Pavan L., Burderi L., Burgay M., Campana S., di Salvo T., Falanga M., Filipović M. D., Freire P. C. C., Hessels J. W. T., Possenti A., Ransom S. M., Riggio A., Romano P., Sarkissian J. M., Stairs I. H., Stella L., Torres D. F., Wieringa M. H., Wong G. F., 2013a, *Nat*, 501, 517
- Papitto A., Torres D. F., Li J., 2013b, *MNRAS*
- Patruno A., Archibald A. M., Hessels J. W. T., Bogdanov S., Stappers B. W., Bassa C. G., Janssen G. H., Kaspi V. M., Tendulkar S., Lyne A. G., 2014, *ApJ*, 781, L3
- Patruno A., Watts A. L., 2012, *ArXiv e-prints*, 1206.2727
- Pretorius M. L., 2009, *MNRAS*, 395, 386
- Radhakrishnan V., Srinivasan G., 1982, *Current Science*, 51, 1096
- Ransom S. M., Eikenberry S. S., Middleditch J., 2002, *AJ*, 124, 1788
- Ransom S. M., Hessels J. W. T., Stairs I. H., Freire P. C. C., Camilo F., Kaspi V. M., Kaplan D. L., 2005, *Science*, 307, 892
- Ray P. S., Abdo A. A., Parent D., Bhattacharya D., Bhattacharyya B., Camilo F., Cognard I., Theureau G., Ferrara E. C., Harding A. K., Thompson D. J., Freire P. C. C., Guillemot L., Gupta Y., Roy J., Hessels J. W. T., Johnston S., Keith M., Shannon R., Kerr M., Michelson P. F., Romani R. W., Kramer M., McLaughlin M. A., Ransom S. M., Roberts M. S. E., Saz Parkinson P. M., Ziegler M., Smith D. A., Stappers B. W., Weltevrede P., Wood K. S., 2012, *ArXiv e-prints*, 1205.3089
- Ray P. S., Ransom S. M., Cheung C. C., Giroletti M., Cognard I., Camilo F., Bhattacharyya B., Roy J., Romani R. W., Ferrara E. C., Guillemot L., Johnston S., Keith M., Kerr M., Kramer M., Pletsch H. J., Saz Parkinson P. M., Wood K. S., 2013, *ApJ*, 763, L13
- Roberts M. S. E., 2013, in *IAU Symposium*, Vol. 291, *IAU Symposium*, pp. 127–132
- Romani R. W., Shaw M. S., 2011, *ApJ*, 743, L26
- Roming P. W. A., Kennedy T. E., Mason K. O., Nousek J. A., Ahr L., Bingham R. E., Broos P. S., Carter M. J., Hancock B. K., Huckle H. E., Hunsberger S. D., Kawakami H., Killough R., Koch T. S., McLelland M. K., Smith K., Smith P. J., Soto J. C., Boyd P. T., Breeveld A. A., Holland S. T., Ivanushkina M., Pryzby M. S., Still M. D., Stock J., 2005, *Space Sci. Rev.*, 120, 95
- Saitou K., Tsujimoto M., Ebisawa K., Ishida M., 2009, *PASJ*, 61, L13
- Sault R. J., Killeen N. E. B., 1998, *The Miriad User’s Guide*. Sydney: Australia Telescope National Facility
- Sazonov S. Y., Revnivtsev M. G., 2004, *A&A*, 423, 469
- Stappers B. W., Archibald A. M., Hessels J. W. T., Bassa C. G., Bogdanov S., Janssen G. H., Kaspi V. M., Lyne A. G., Patruno A., Tendulkar S., Hill A. B., Glanzman T., 2013, *ArXiv e-prints*, 1311.7506
- Takata J., Li K. L., Leung G. C. K., Kong A. K. H., Tam P. H. T., Hui C. Y., Wu E. M. H., Xing Y., Cao Y., Tang S., Wang Z., Cheng K. S., 2013, *ArXiv e-prints*, 1312.0605
- Tam P. H. T., Kong A. K. H., Li K. L., 2013, *The Astronomer’s Telegram*, 5652, 1
- Thorstensen J. R., Armstrong E., 2005, *AJ*, 130, 759
- Wang Z., Archibald A. M., Thorstensen J. R., Kaspi V. M., Lorimer D. R., Stairs I., Ransom S. M., 2009, *ApJ*, 703, 2017
- Wijnands R., van der Klis M., 1998, *Nat*, 394, 344
- Wilson W. E., Ferris R. H., Axtens P., Brown A., Davis E., Hampson G., Leach M., Roberts P., Saunders S., Koribalski B. S., Caswell J. L., Lenc E., Stevens J., Voronkov M. A., Wieringa M. H., Brooks K., Edwards P. G., Ekers R. D., Emonts B., Hindson L., Johnston S., Maddison S. T., Mahony E. K., Malu S. S., Massardi M., Mao M. Y., McConnell D., Norris R. P., Schnitzeler D., Subrahmanyan R., Urquhart J. S., Thompson M. A., Wark R. M., 2011, *MNRAS*, 416, 832
- Woudt P. A., Warner B., Pretorius M. L., 2004, *MNRAS*, 351, 1015